Impact of Autotransformer Inrush Currents on Differential Protection Operation

Bozidar Filipovic-Grcic, Marijan Perkovic, Nina Stipetic

***Abstract*— One of the main causes for incorrect operation of the transformer relay protection are inrush currents. The transient inrush currents occur when energizing the unloaded transformer, and it is a consequence of the transformer core saturation.**

This paper presents an analysis of transients caused by energization of three-phase autotransformer 300 MVA, with rated voltages 400/115/10.5 kV. Using the EMT software with parametric toolbox, a large number of simulations is performed to show the impact of model parameters on the amplitude and duration of inrush currents as well as the probability of differential current 2nd harmonic amplitude occurrence. Based on the simulation results, the optimal differential protection settings are determined, and the probability of a false relay protection operation is determined.

***Keywords*: autotransformer, inrush current, differential protection, parametric modelling**

I. Introduction

TRANSFORMER energization is a switching operation which causes inrush transient currents with amplitudes that are comparable to short-circuit current amplitudes, (8-15)I_n. If the transient inrush current lasts longer than the differential relay operating time of approximately 30 ms, the differential protection is activated. Since the energization is a standard switching operation, the relay protection must not recognize it as a fault resulting in a false tripping of circuit breaker (CB) and switching off transformer. Harmonic analysis of inrush currents shows its specifically high content of 100 Hz current, which is why the 2nd harmonic is used for adjusting the selectivity for relay tripping [1].

Identification of the inrush current is a prominent research topic, yielding the literature based on theoretical analysis, software simulations, inrush current identification and reduction [2]-[11]. Factors that influence the inrush current amplitude and its duration are CB switching time, remanent flux in the magnetic core, network short-circuit power and network voltage [2],[7]. The differential relay receives measured currents from the secondary windings of current transformers (CTs) placed at the beginning and at the end of the protected object (transformer, motor, generator), and processes the obtained signal, firstly performing analog-to-digital conversion of currents measured on the secondary of CTs [1].

B. Filipovic-Grcic and N. Stipetic are with University of Zagreb, Faculty of Electrical Engineering and Computing, 10000 Zagreb (e-mail of corresponding author: bozidar.filipovic-grcic@fer.hr).
M. Perkovic is with E.ON Solar d.o.o., Capraska 6, 10000 Zagreb, (e-mail: marijan.perkovic@eon.hr)

Paper submitted to the International Conference on Power Systems Transients (IPST2023) in Thessaloniki, Greece, June 12-15, 2023.

Therefore, the analysis of the inrush currents' influence on the differential protection operation requires modelling of both the primary and secondary circuit.

The influence of one variable parameter on inrush current can be evaluated by numerous individual simulations. However, such an approach to transient analysis with multiple influential parameters is impractical and time-consuming. Therefore, the most unfavourable cases are most often simulated, but their occurrence probability in practice is small. This paper shows a possibility of parametric modelling of transformer energization event, showing the results of 300 automatically generated EMT simulations. Based on the simulation results, individual model parameters' influence on the amplitude and duration of the inrush current is analysed, and the occurrence probability of the 2nd harmonic content in the differential current is determined.

II. EMTP Model Built for the Differential Protection Study

In [12], the transformer energization modelling guidelines are given. Fig. 1 shows a model used for simulating an energization of unloaded transformer 400/115/10.5 kV and differential protection operation analysis. The energization is performed by switching a CB on the 400 kV side.

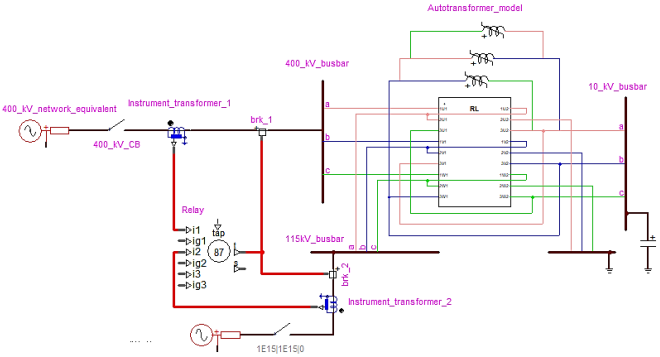

Fig. 1. EMTP model used for differential protection analysis upon energization of an unloaded transformer

The transformer is modelled based on short-circuit and open-circuit data, using a BCTRAN model, with addition of nonlinear inductances for representing the iron core saturation. The nonlinear inductances are connected to terminals of the tertiary winding which is the closest to the core. For cylindrical coil construction, it can be assumed that the flux in the windings closest to the core will mostly go through the core, since there should be very little leakage. This winding is usually the tertiary winding in three-winding transformers, and in such cases, it is therefore best to connect the nonlinear inductance across the tertiary terminals. Since measurements of the magnetizing current are usually performed up to the "knee-point"

corresponding to 1.1-1.2 p.u. of the rated voltage, it is necessary to determine the value of the inductance in the saturation region. Typical values for air-core inductances are $2L_k$ for two-winding transformers with separate windings, or (4-5)L_k for autotransformers, where L_k represents short-circuit inductance [12], [13]. Saturation RMS current-voltage characteristic was obtained from transformer manufacturer and converted into an instantaneous flux-current saturation curve using nonlinear inductance data function. On the 400 kV side of autotransformer, CTs are modelled taking into account saturation curve of protection core (class 5P30) [14]. Transients involving large current amplitudes (caused by energization or faults) may lead to CT saturation, which results in distortion of current on CT secondaries. This can lead to misinterpretation and false tripping of relay protection devices. For this reason, CT magnetization curve needs to be considered in CT model. The data used for modelling of autotransformer and CTs are given in Appendix I. The secondary winding of the protection core is connected to a differential relay model available in the protection toolbox, which contains the differential protection function whose settings can be modified by user. The differential relay model in EMTP is robust and, at first level, it contains current signal processing, which simulates the current signal processing in reality. After the signal acquisition and an anti-aliasing filter, the filtered current signal is sampled and sent to discrete Fourier transform algorithm to obtain the phasors, rms and sequence values of current at different frequencies. After this step, the processed current is ready for differential protection algorithm. The differential protection can use 3 CT inputs and different shapes of 2-slope characteristics and restraint options. The 400 kV network equivalent is modelled as voltage source behind short-circuit impedance, based on three-phase and single-phase short-circuit power of 10 GVA and 3 GVA, respectively.

III. Results of Individual Time Domain Simulations Considering the Effect of Remanent Flux

Remanent flux in the core of power transformer is an important parameter affecting inrush currents. It can have different values during power transformer operation. Two cases are considered: with and without remanent flux in the core of the power transformer. Transformer energization is simulated in a case of 400 kV CB switching at 15 ms, corresponding to voltage zero-crossing in phase A.

A. Case 1 – Simulation without remanent flux

Fig. 2 shows the inrush currents in all phases, for transformer energization at 15 ms corresponding to voltage zero-crossing in phase A, and without remanent flux in the transformer core. In this case, the inrush current amplitude is highest in the phase A. This is expected since the energization is done at a time instance corresponding to the voltage zero-crossing and maximum magnetic flux in phase A.

A. Case 2 – simulation with remanent flux and analysis of differential protection operation

Fig. 3 shows the inrush currents in all phases for energization at 15 ms, with remanent magnetic flux in the power transformer

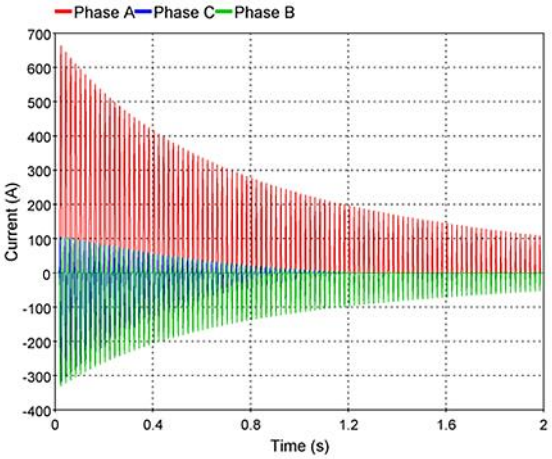

Fig. 2. Inrush currents in case of energization at voltage zero-crossing in phase A, without remanent flux in the core

core. Phase A has remanent flux of 80%, and phase C -80% of the rated flux. The inrush currents in phases A and C are higher than the inrush current in phase B, which is expected due to remanent fluxes and the switching time instance.

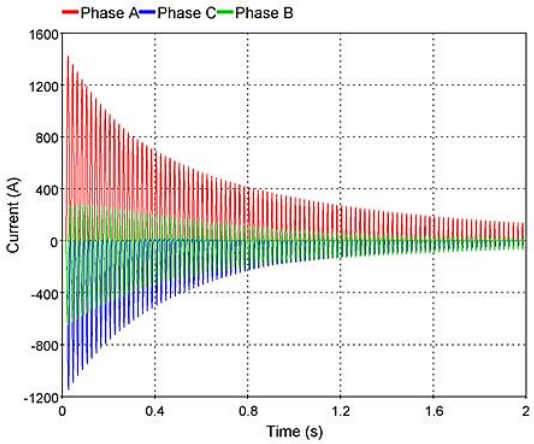

Fig. 3. Inrush currents in case of energization at voltage zero-crossing in phase A, with remanent flux in the core

For this simulation, the differential protection operation is analysed. The content of the 2nd harmonic in the differential current starts to be continuously calculated in the protection relay model when the differential current reaches a pre-set value. As shown in Fig. 4, the 2nd harmonic share increases with the simulation time [11]. The lowest value of this 2nd harmonic share during the time when the protection can be triggered is relevant for setting the differential protection. In this case, according to Fig. 4, the lowest 2nd harmonic shares in each phase A, B and C are 7.2%, 33.93% and 17.72%, respectively. Having an insight into the actual 2nd harmonic content in the differential current enables the adjustment of relay settings, so non-selective tripping of the relay can be avoided.

In the following simulations, the differential protection operation is observed. For case 2, inrush current waveforms in phase A are observed when differential protection blocking is set to 5% and 10% od 2nd harmonic content. According to Fig. 5, the lowest 2nd harmonic content is 7.2%, successful differential protection blocking is expected for a setting of 5%,

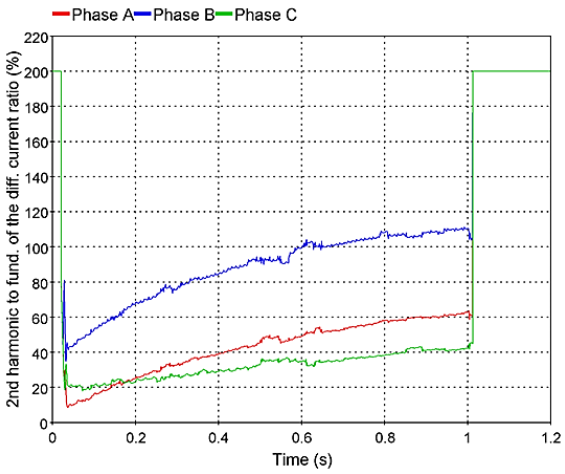

Fig. 4. 2nd harmonic content in the differential current in the case 2

and non-selective differential relay tripping is expected when the maximum allowable ratio is set to 10 %.

Fig. 5 shows the current waveform in phase A and tripping signals when the transformer is energized and blocking of differential protection is set to 5% of 2nd harmonic content. Fig. 6 shows the same, but for setting of 10 %.

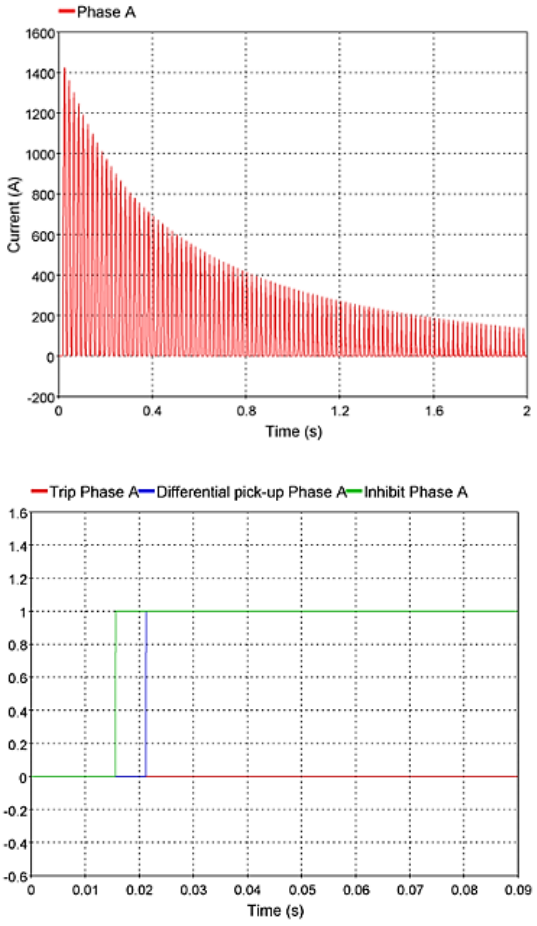

Fig. 5. Inrush current in phase A, differential protection blocking is set to 5% of the 2nd harmonic content. The tripping is inhibited due to the 2nd harmonic content even when the pick-up setting reacts. The breaker tripping is prevented.

According to the waveform in Fig. 5, the differential protection is not activated, and the inrush current is not interrupted due to the successful blocking of the differential protection based on 5% of 2nd harmonic content in the differential current. According to the previous simulation, the 2nd harmonic content in the differential current is always greater than 5%. On the other hand, in Fig. 6, the inrush current in phase A is interrupted after less than 40 ms from the energization instant. The differential protection was not successfully blocked because the 2nd harmonic content in the differential current is lower than 10%. These simulations confirmed that blocking of the differential relay operation occurs as expected. However, inrush currents in practice are affected by numerous factors which have random behaviour. These factors can be considered by performing larger number of parametric simulations [15], which is shown in the next paragraph.

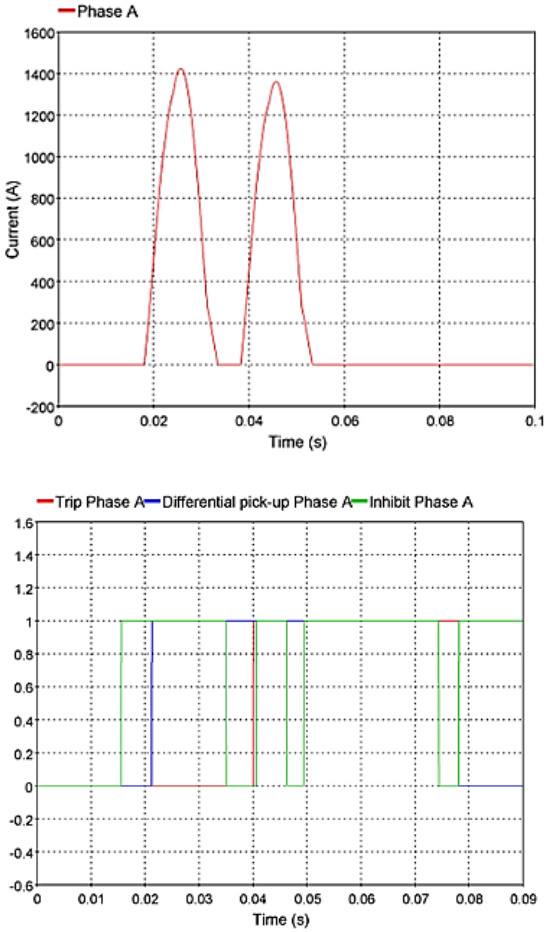

Fig. 6. Inrush current in phase A, differential protection blocking is set to 10% of the 2nd harmonic content. The tripping signal is activated at 40 ms due to high setting of 2nd harmonic blocking.

IV. Parametric Approach to Calculation of Inrush Currents

A. Parametric modelling of transformer energization

Existing parametric toolboxes in EMT softwares are convenient for parametric and stochastic modelling for probability related studies. It enables to monitor chosen quantities and analyse their dependence on the other influential parameters. Energization of an unloaded transformer is a stochastic phenomenon that depends on the value of the AC

voltage at switching time instant in each individual phase [15]. Due to the inertia of the CB drive mechanism, and the scattering of the CB switching time, a parametric approach for simulating the energization is reasonable and recommended. The interruption in phase A can be modelled as uniform probability distribution within one power-frequency period of 20 ms (1). The time difference for interruption in other two phases can be modelled by normal distribution according to (2), to include the CB mechanism time dissipation up to 5 ms. Finally, the interruption time in phases B and C differs from interruption time in phase A due to this time dissipation, as defined in (3).

$$t_A \in [n, n+1] \cdot 20 \text{ ms}, n \in N, \quad (1)$$

$$t_{B,diss} \text{ and } t_{B,diss} \sim N(0,5 \text{ ms}), \quad (2)$$

$$t_B = t_A + t_{B,diss} \text{ and } t_C = t_A + t_{C,diss}, \quad (3)$$

where $t_{A,B,C}$ are interruption times of the CB in phases A, B and C, and $t_{B,diss}$, $t_{C,diss}$ are time dissipations of interruption times for phases B and C. The exact value of the remanent flux in the core is unknown. The remanent flux in phase A can be described as (4), and its amplitude and angle can be modelled as uniform distributions according to (5). In phases B and C, the remanent flux is simply phase-shifted by 120°, as shown in (6)-(7).

$$\phi_A = \phi_{A,amp} \cdot \cos(\alpha), \quad (4)$$

$$\phi_{A,amp} \in [0, 0.8 \text{ p.u.}], \ \alpha \in [0°, 360°], \quad (5)$$

$$\phi_B = \phi_{A,amp} \cdot \cos(\alpha - 120°), \quad (6)$$

$$\phi_C = \phi_{A,amp} \cdot \cos(\alpha + 120°), \quad (7)$$

where α is the angle corresponding to interruption time in phase A, and it is dependent on interruption time t_A, while $\phi_{A,B,C}$ are the remanent fluxes in phases A, B and C. Remanent flux in the CT core depends on its protection class. Class P protection cores can have a remanent flux of up to 90% of saturation flux, while the remanent flux is negligible for TPZ protection cores. The network voltage varies within certain limits, and for the 400 kV network in this analysis, the 360-420 kV range was considered. The network impedance depends on certain network topology and short-circuit power; therefore, the equivalent network impedance also varies within known limits.

B. Parametric simulation results

300 simulations are performed considering variations in time instances of energization, remanent fluxes, short-circuit power and network voltage. The number of simulations was chosen based on probability of 2nd harmonic occurrence in the studied case. After 300 simulations, the 2nd harmonic occurrence probability stabilized. This convergence can be continuously tracked within the parametric toolbox and serves for easier determination of needed number of simulations in any case. Fig. 7 shows the amplitudes of inrush currents depending on the time instance of energization. The sinusoidal form can be observed, with maximal values corresponding to time instances when the voltage is close to zero. Controlled switching of CB at voltage maximum would significantly reduce the amplitudes of inrush currents [16],[17]. In controlled switching case, the inrush current amplitude would depend on the remanent flux in the power transformer core. Fig. 8 shows the amplitudes of inrush currents depending on the remanent flux in phase A.

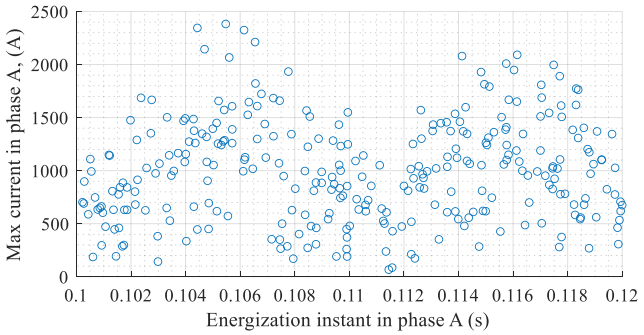

Fig. 7. Inrush currents' amplitudes for different switching instants in phase A

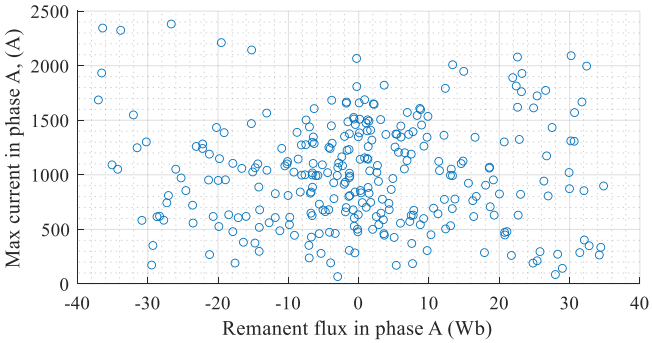

Fig. 8. Inrush currents' amplitudes for different remanent fluxes in phase A

The remanent flux can increase or decrease the inrush current amplitude, depending on the polarity of the voltage in first half-cycle after switching. Since the parametric simulation is performed using random distribution of parameters, until the convergence of 2nd harmonic is reached, this dependence is not directly seen from Fig 8. However, the highest current values occur at margins of defined remanent flux of -0.8 and 0.8 p.u. Fig. 9 shows the results of a few time domain simulations for clear view of remanent flux influence on inrush current.

Three-phase short-circuit power and the voltage in the network also affect the maximum value of the inrush currents, but this influence is not comparable to the influence of the switching time instant or remanent flux. By increasing the power of the three-phase short circuit, the equivalent network has lower impedance, which results in inrush current increase. As the network voltage increases, the magnetic flux inside the core of the transformer increases. An increase in magnetic flux leads to greater core saturation and higher inrush currents.
Regarding the 2nd harmonic content in inrush currents, results in Fig. 10 show that 2nd harmonic content in the differential current decreases with increase of inrush current amplitudes.

Aside from analysis of the mutual dependencies of certain parameters, it is possible to calculate the occurrence probabilities of the 2nd harmonic contents in the differential current. The cumulative probability distribution is given in Fig 11. In 10% cases, the 2nd harmonic content in differential current was lower than 20%.

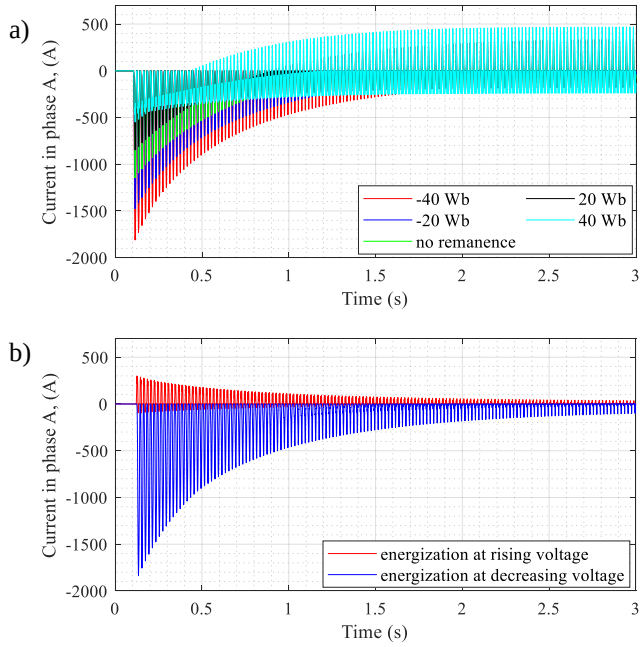

Fig. 9. Inrush current amplitude in phase A in case of: a) same time instance of energization and different remanent fluxes, b) same remanent flux and different time instance of energization

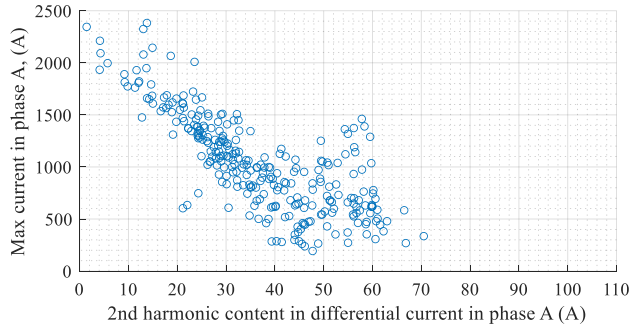

Fig. 10. Dependence of 2nd harmonic content in the differential current and inrush current amplitude

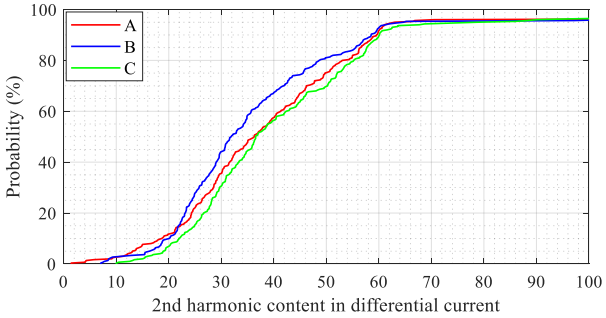

Fig. 11. Probability distribution of the 2nd harmonic content in the differential current for phases A, B and C

In practice, the experience has shown that the inrush currents contain at least 20% of 2nd harmonic, while the percentage is never higher than 5% in overcurrents caused by transformer internal faults. Thus, in practice, a value of 15-30% is usually used to block the differential protection operation [1], [18].

The probabilities of non-selective differential protection operation are additionally analysed on this example, for the blocking setting of 15%, 20%, and 30%. The results are given in Table I. The probabilities are calculated based on 300 simulations, which is enough to achieve convergence of 2nd harmonic occurrence probabilities.

TABLE I
TRIPPING PROBABILITIES IN EACH PHASE FOR DIFFERENT RELAY SETTING

2nd harmonic content	15% setting	20% setting	30% setting
Phase A	7.0%	13.5%	37%
Phase B	6.5%	14%	32%
Phase C	3.0%	7.5%	44%

Setting of 15% to block the protection operation would result in non-selective triggering for less than 10% of random switching cases (without applying CB controlled switching). This analysis can be used to determine the lowest possible 2nd harmonic content in all phases, which is a valuable information for differential protection setting. Using this information, all non-selective tripping could be avoided. In this case, for phase B, the 2nd harmonic content in the differential current is never less than 7%. If the relay is parameterized to block the protection operation for the 2nd harmonic share in the differential current higher than 7%, there would be no non-selective activation of the relay. This value is well below the minimum recommended value of 15%. When the parametric calculations of energization result in very low values of 2nd harmonic content in differential currents, the analysis of harmonic content in fault currents could be additionally analysed for comparison and confirmation that such low setting would not detract the primary function of the differential protection [19]-[23].

V. CONCLUSION

A simulation of 400/110/10.47 kV autotransformer energization is performed. The instrument transformer and the secondary circuit with the relay were modelled in detail. The performed simulations have shown the expected differential protection behaviour. The possibility of parametric modelling and statistical analysis using the parametric toolbox is shown.

The simulations confirmed that the inrush current amplitudes are affected mostly by the switching time instant and the remanent flux in the transformer core. The remanent flux can increase or decrease the inrush current amplitudes, depending on the increasing or decreasing voltage cycle after the switching. The increase in network voltage or short-circuit power increases the amplitude of inrush currents. The 2nd harmonic content is lower in the case when differential currents have higher amplitudes.

In practice, amounts of 15-30% of the 2nd harmonic are used to block the differential relay operation, with the remark that values less than 15% are not recommended, since lower inrush restraint setting may impact the tripping time of the differential element for fault conditions. For the studied case, it was shown that the setting of 15% can lead to a certain number of non-selective relay tripping. Generally, parametric simulations of transformer energization can be used to find the lowest 2nd harmonic contents in differential currents for the exact setting of differential current protection blocking. If the statistically obtained lowest 2nd harmonic content in differential current is

lower than 15%, additional simulations of internal faults and energizations of a transformer with an existing internal fault should be performed. The parametric approach can also be used for fault simulations. Comparison of 2nd harmonic content in differential overcurrents caused by energization and those caused by faults would confirm the optimal setting and that it will not disrupt, nor the basic function of differential protection - elimination of internal fault in the transformer, nor the non-selective tripping in case of energizations. Based on parametric simulations of energization and faults, it is possible to determine the protection setting that is sufficient to make the probability of transformer failure acceptably low. The determined optimal differential protection setting would in the end contribute to the increase of the availability and safety of the power transformer.

APPENDIX I

TABLE II
AUTOTRANSFORMER DATA

Rated voltage	400/115/10.47 kV		
Rated power	300/300/100 MVA		
Connection	Yna0d5		
Core type	Five-limb-core		
Short circuit data		U_k (%)	P_k (kW)
	HV_MV (300 MVA)	12.23	487
	HV-LV (100 MVA)	8.68	152
	MV-LV (100 MVA)	3.37	141
Open circuit data	I_0=0.041 %		
	P_0=90.8 kW		

TABLE III
400 KV CURRENT TRANSFORMER DATA

Type	AGU - 420
I_{prim}/I_{sec}	1600/1 A
Rated power	30 VA
Class	5P30
ALF	35.84

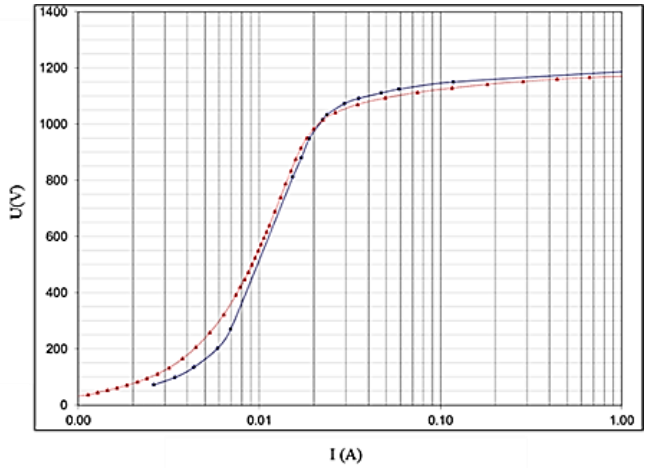

Fig. 12. CT Saturation curve – red curve represents measured characteristic obtained with Omicron CT Analyzer; blue curve represents characteristic calculated considering protection core material and geometry.

VI. REFERENCES

[1] Christophe Preve, "Protection of Electrical Networks", ISTE 2006.

[2] R. Gopika, D. Sankar, "Study on Power Transformer Inrush Current", *IOSR Journal of Electrical and Electronics Engineering*

[3] Hamilton R., "Analysis of transformer inrush current and comparison of harmonic restraint methods in transformer protection", *IEEE Trans Ind Appl*, 49 (4) (2013)

[4] Xianggen Yin, Wenbin Cao, Yuanlin Pan, "Inrush current characteristic of high impedance transformers and its impact on protective relays", *Power Syst Prot Control*, 46 (20) (2018)

[5] Cui Y., Abdulsalam S.G., Chen S., Xu W., "A sequential phase energization method for transformer inrush current reduction—part I:Simulation and experimental results", *IEEE Trans Power Deliv*, 20 (2) (2005), pp. 943-949

[6] Peng Fang, Gao Houlei, Liu Yiqing, "Transformer sympathetic inrush characteristics and identification based on substation-area information", *IEEE Trans Power Deliv*, 33 (1) (2018)

[7] Ren Hongtao, "Simulation analysis of inrush current in no load closing of transformer in Hydropower Station", *Energy Reports*, Volume 7, Supplement 7, 2021, Pages 1175-1181,ISSN 2352-4847

[8] Haidar Samet, Maral Shadaei, Mohsen Tajdinian, "Statistical discrimination index founded on rate of change of phase angle for immunization of transformer differential protection against inrush current", *International Journal of Electrical Power & Energy Systems*, Volume 134, 2022

[9] Heba Beder, Ebrahim A. Badran, Ahmed Y. Hatata, Magdi M. Elsaadawi, "Inrush current detection enhancement for legacy overcurrent relays in north delta electric distribution company", *Electric Power Systems Research*, Vol. 201, 2021

[10] Mohsen Tajdinian, Haidar Samet, "Application of probabilistic distance measures for inrush and internal fault currents discrimination in power transformer differential protection", *Electric Power Systems Research*, Volume 193, 2021

[11] Raidson Jenner Negreiros Alencar, Ubiratan Holanda Bezerra, André Maurício Damasceno Ferreira, "A method to identify inrush currents in power transformers protection based on the differential current gradient", *Electric Power Systems Research*, Volume 111, 2014

[12] CIGRE Technical brochure 568: Transformer Energization in Power Systems: A Study Guide, WG C4.307, 2014

[13] Dommel, H. W.: Electromagnetic Transient Program (EMTP), "Theory Book", Bonneville

[14] IEC 61869-2:2012 Standard | Instrument transformers - Part 2: Additional requirements for current transformers.

[15] M. Martinez, P. Poujade, "Transformer Energization Study Case with PAMSUITE", *EMTP User Conference*, Perpignan 2019.

[16] Ramón Cano-González, Alfonso Bachiller-Soler, José Antonio Rosendo-Macías, Gabriel Álvarez-Cordero, "Controlled switching strategies for transformer inrush current reduction: A comparative study", *Electric Power Systems Research*, Volume 145, 2017

[17] Brunke J.H., Frohlich K.J., "Elimination of transformer inrush currents by controlled switching–part I: Theoretical considerations", *IEEE Trans Power Deliv*, 16 (2) (2001)

[18] Network protection & automation guide, edition May 2011, Alstom Grid

[19] M. Rasoulpoor, M. Banejad, "A correlation based method for discrimination between inrush and short circuit currents in differential protection of power transformer using discrete wavelet transform: Theory simulation and experimental validation", *Int. J. Elect. Power Energy Syst*., 51 (Oct. 2013), pp. 168-177

[20] A. Sahebi, H. Samet, T. Ghanbari, "Identifying internal fault from magnetizing conditions in power transformer using the cascaded implementation of wavelet transform and empirical mode decomposition", *International Transactions on Electrical Energy Systems* (2018), p. 2485

[21] S.R. Samantaray, P.K. Dash, "Decision Tree based discrimination between inrush currents and internal faults in power transformer", *International Journal of Electrical Power & Energy Systems*, Volume 33, Issue 4, 2011

[22] Maya P., S. Vidya, Roopasree K., K.P. Soman, "Discrimination of Internal Fault Current and Inrush Current in a Power Transformer Using Empirical Wavelet Transform", *Procedia Technology*, Volume 21, 2015

[23] F. Mieske, K. Solak, W. Rebizant, S. Schneider, "Advanced transformer protection to secure discriminating internal faults from inrush currents in inverter-based generation networks", CIGRE Paris Session 2022